Assessing the Role of Initial Imperfections in Cylinder Buckling Using 3D Printing

by

Haocheng Yang

Department of Mechanical Engineering and Materials Science
Duke University

Date:_______________________
Approved:

____
Lawrence N. Virgin, Supervisor

____
Brian P. Mann

____
Tomasz A. Hueckel

Thesis submitted in partial fulfillment of
the requirements for the degree of
Master of Science in the Department of
Mechanical Engineering and Materials Science in the Graduate School
of Duke University

2019

ABSTRACT

Assessing the Role of Initial Imperfections in Cylinder Buckling Using 3D Printing

by

Haocheng Yang

Department of Department of Mechanical Engineering and Materials Science
Duke University

Date:_______________________
Approved:

____
Lawrence N. Virgin, Supervisor

____
Brian P. Mann

____
Tomasz A. Hueckel

An abstract of a thesis submitted in partial
fulfillment of the requirements for the degree
of Master of Science in the Department of
Mechanical Engineering and Materials Science in the Graduate School of
Duke University

2019

Abstract

This thesis assesses the role of several types of designed initial imperfection on the buckling behavior of 3D printed cylindrical shells through experimental method. The buckling loads and paths are given by the axial compression tests while the lateral force-displacement relationships are given by the lateral poking tests at first. Then the influences of designed imperfections on them are discussed. The test results show that the effect of designed initial imperfections in this thesis might be overridden by other unpredictable imperfections. Poking tests can provide some information on the buckling loads and paths that is difficult to obtain through compression tests. The designed buckling mode shapes imperfections may generate bigger influences than the designed imperfections as shown in this thesis.

Contents

List of Tables

List of Figures

Acknowledgements

I would first like to thank my advisor Dr. Lawrence Virgin for letting me join his lab and conduct my research. His guidance on the basic knowledge, experiment plan, result interpretation and writing strongly helped me move forward in the right the direction.

I would like to thank Patrick McGuire, Eric Stach and Richard Glisson for their guidance on the experiment settings and the operation of printing and testing devices.

I would also like to thank Yue Guan and Yawen Xu, two fellow doctoral students in my lab, for their perspectives and suggestions on my research.

1. Introduction

The buckling of cylindrical shells has been an important research topic for years. The shells here and in the study of this thesis are characterized by the same magnitude between heights and outside diameters and the far less magnitude of thicknesses. To estimate the buckling loads of such structures, comprehensive theoretical and experimental work has been completed. The classical solution based on the linear theory, which is related to the size of the cylinder and the mechanical properties of its material, was obtained in the early twentieth century, but it could not be verified by experiments [1]. The scatter of experimental buckling loads was shown in many references such as [2] (adopted here in Fig.1) and [3] and these loads were evidently lower than the classical result.

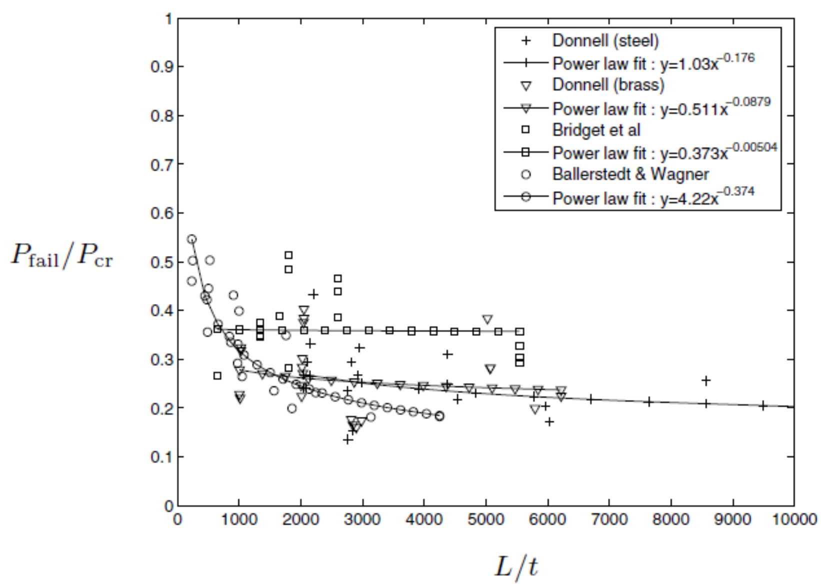

Figure 1: The scatter of buckling loads adopted from [2]

The discrepancies between the theoretical and experimental results drew attention to the full buckling behavior besides the buckling load. [4] summarizes the process of revealing and interpreting the snap-through buckling behavior of cylindrical shells. The lower buckling load P_L and the Maxwell load P_M were described and a simplified buckling diagram is adopted here in Fig.2. [5] also reported a schematic representation of the postbuckling response based on many studies adopted here in Fig.3.

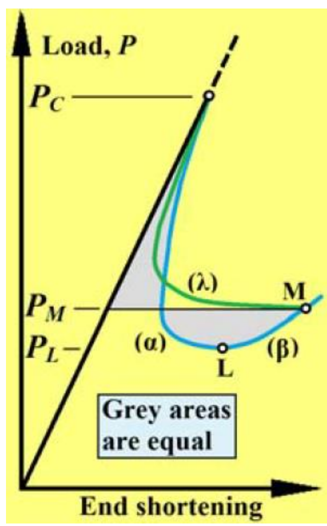

Figure 2: The simplified buckling path adopted from [4]

Of particular interest in [4] was the innovative poking test, where the cylinder was subject to a fixed axial load at first and then poked laterally. In this way the lateral force-displacement relationship at the poking point could be obtained and then used to measure the energy barrier against buckling to identify the unstable state in the buckling when the prescribed axial load is higher than P_L. Comparing with the traditional axial compression test, poking test is a non-destructive method to investigate the buckling load and path [6]. [7] did poking tests on commercial aluminum cans and demonstrated the underlying stability landscape of cylindrical shells as shown in Fig.4.

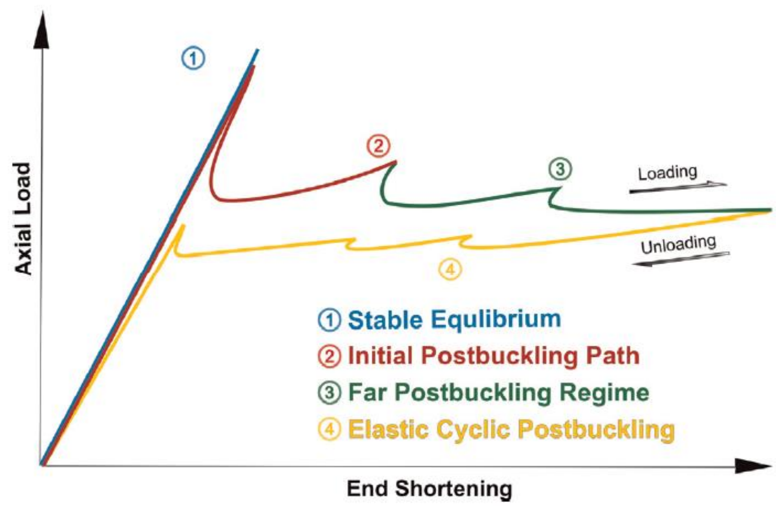

Figure 3: The schematic postbuckling path adopted from [5]

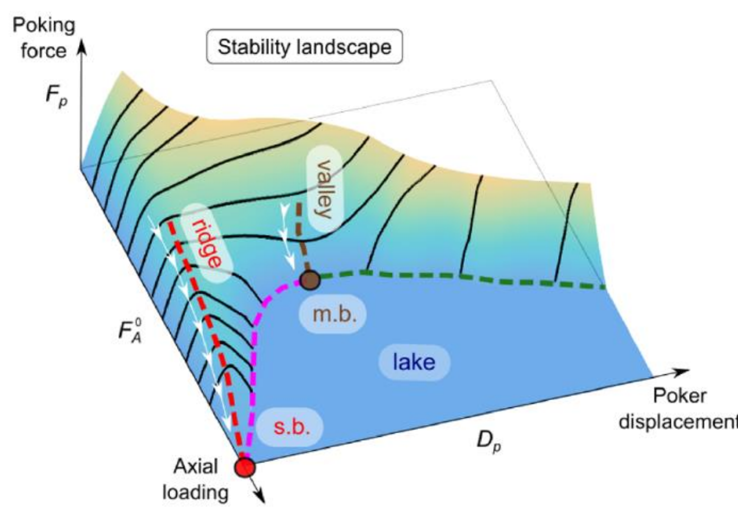

Figure 4: The stability landscape of cylinder buckling adopted from [7]

Among all research on the buckling of cylindrical shells, initial imperfections were frequently the focus. [8] mentioned the significant reduction of buckling loads caused by imperfections and implied that imperfections may explain the differences between the actual and theoretical results. [1] reported the theoretical buckling path of an imperfect shell and [9] theoretically studied the influence of imperfections on buckling loads. [5] chose the buckling mode shapes gained from numerical eigenvalue analyses as the initial imperfections and conducted simulations and axial compression tests on the buckling paths.

The aim of this thesis is introducing the poking test to assess the influences of several types of initial imperfection on the buckling behavior of cylindrical shells. The influences on both the buckling load and path given by compression tests and the shape of the lateral force-displacement relationship given by poking tests will be described. All cylinders were 3D printed so that the shapes of imperfection could be easily prescribed.

2. Experiment Setup and Process

This section describes the preparation work for axial compression and lateral poking tests and the test process.

2.1 Basic Size

The designed size of the standard cylindrical shell without any prescribed initial imperfections, which is defined as the basic size, was mainly determined by the space and cost of 3D printing and the capacity of measuring devices. After many trials, the basic size was chosen as 200 mm height, 115.7 mm outside diameter and 0.7 mm thickness. Standard cylinders in this size and imperfect cylinders similar to this size can be printed with limited time, materials and tray consumption. Moreover, all peak loads on such cylinders in compression and poking tests were below the capacity of the materials testing machine and load cell.

2.2 Shapes of Initial Imperfection

The initial imperfections in this thesis were generated by half period sine-wave generatrixes with 1 mm and 5 mm designed amplitudes. Imperfect cylinders with these two generatrix amplitudes are denoted as Ap-1 and Ap-5. Consequently, these imperfect cylinders had the same designed height and shell thickness with standard cylinders, but only swelled to some degree. The outside diameter of the top and bottom surface was the same as that in the basic size. The SolidWorks model of Ap-5 is shown in Fig.5.

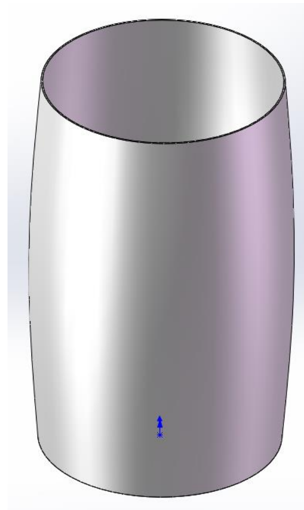

Figure 5: The software model of Ap-5

2.3 Quality of 3D Printing

The 3D printer used to print all cylinders was Fortus 250mc, with ABS*plus* P-430 thermoplastic and a 0.007 inch layer resolution. Three cylinders of standard, Ap-1 and Ap-5 were printed in each shape. Two of each were used in compression tests to examine the repeatability and the rest were used in poking tests. The actual sizes of these nine cylinders are listed in Table.1. The heights H were measured by ruler while the outside diameters D and thicknesses t were measured by digital caliper. Note that D and t of imperfect cylinders were not measured due to the difficulty caused by their shapes. The amplitudes of generatrix A were also not measured.

It can be seen from the results of H that the precision of printing is high and the accuracy is not affected by the shape of the cylinder. Based on this observation it might be concluded that D and t of all imperfect cylinders also approach that of standard cylinders. In this way D is close to the basic size while t is about 10% bigger. So overall the printing quality is high for H and D while low for t. The quality for A cannot be clearly determined.

Table 1: Actual sizes of cylinders

Use	Sample	H (mm)	D (mm)	t (mm)
Compression tests	Standard	200.0	115.36	0.77
	Standard	200.0	115.42	0.75
	Ap-1	200.5		
	Ap-1	200.0		
	Ap-5	200.2		
	Ap-5	200.1		
Poking tests	Standard	200.0	115.54	0.79
	Ap-1	200.0		
	Ap-5	200.0		

2.4 Compression Tests

The goal of the compression tests is to obtain the buckling loads and paths of the cylinders. They also help to decide the prescribed axial loads of interest for the poking tests.

The materials testing machine used in the compression tests was Test Resources 830LE-AT with an axial loading capacity of ±50 kN. The boundary conditions were provided by two steel boards with circular V-shape grooves matching D in the basic size. Thus, this boundary condition is similar to a pinned-pinned condition. The board placed on the top of cylinders added an extra 28.8 N load to them. These settings are shown in Fig.6.

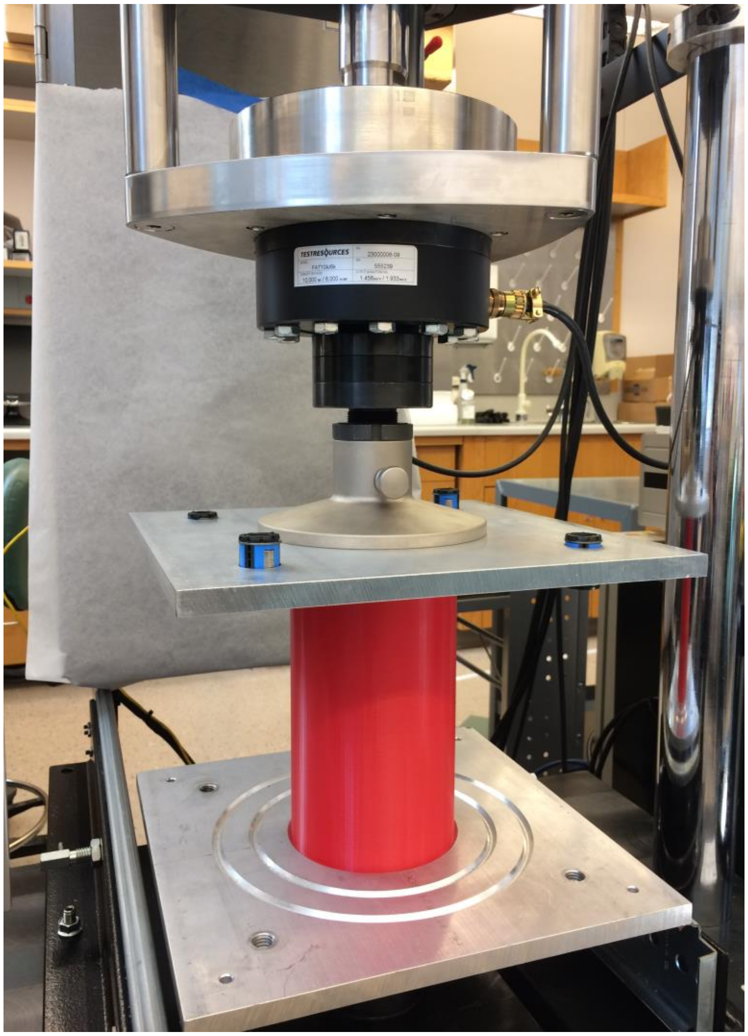

Figure 6: Settings of the compression test

In the actual operation, the position of the top end plate was adjusted as close as possible to the top board based on the load reading at first. Next the test started and the top end plate moved down in a 0.01 mm/s speed for a prescribed displacement to apply load and then moved up in the same speed back to the original position to unload. The buckled cylinder in one test before unloaded is shown in Fig.7.

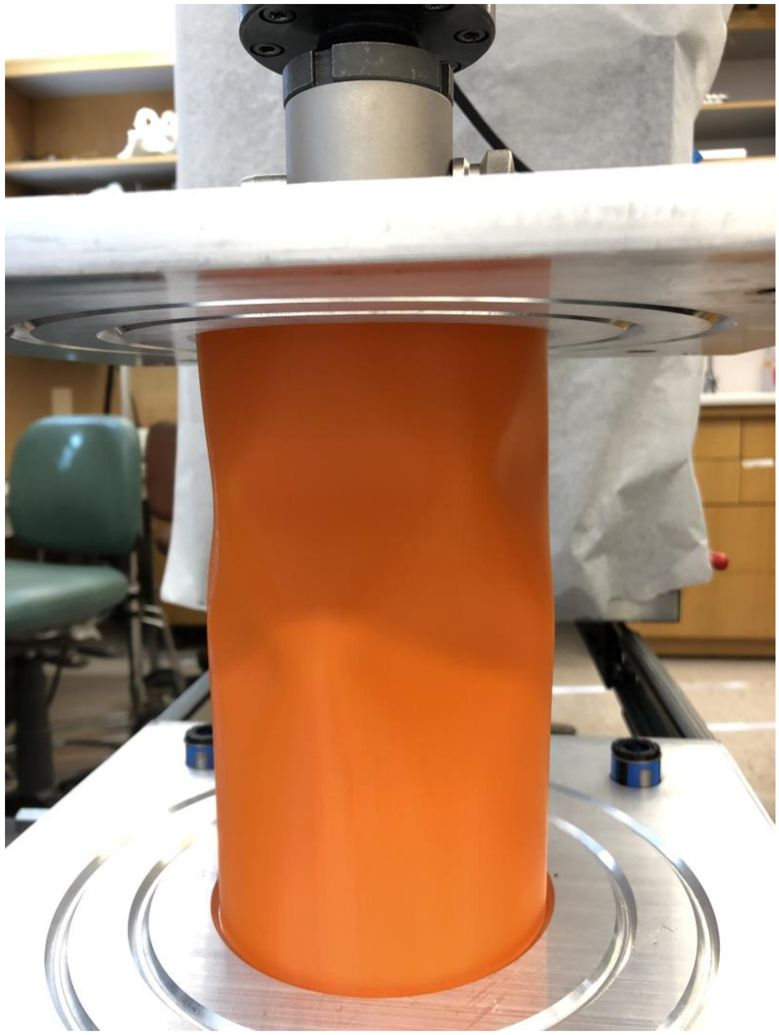

Figure 7: The buckling shape of a cylinder

2.5 Poking Tests

Based on the results of compression tests, poking tests can be conducted to gain the lateral force-displacement relationships of cylinders for the influence evaluation.

The materials testing machine was still needed to provide fixed axial loads. The position control device BISLIDE made by Velmex, Inc. was fixed next to the cylinders and the Omega DFG35-10 load cell was attached to BISLIDE through a 3D printed board.

In this way the load cell could move in a certain speed to implement a displacement control loading scheme. The load cell has a 50 N capacity and 0.05 N resolution. These settings are shown in Fig.8.

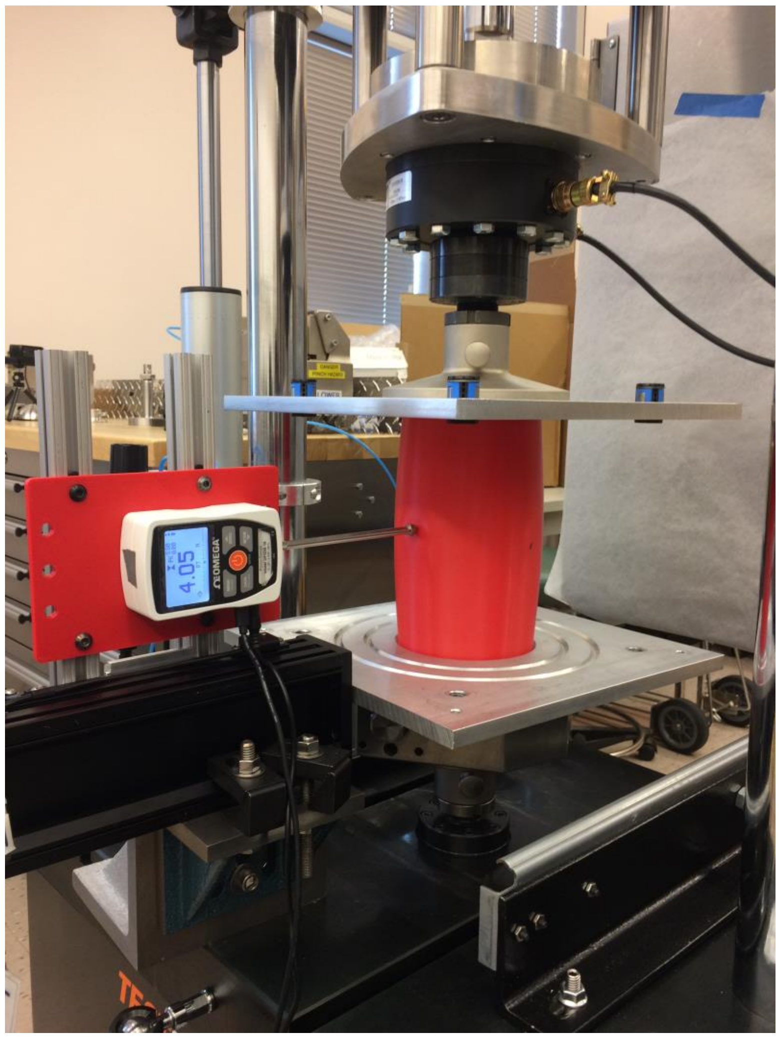

Figure 8: Settings of the poking test

In the actual operation, the prescribed axial loads were applied in a 5 N/s speed and maintained at first. Next the position of the load cell was adjusted as close as possible to the cylinders based on the load reading. The software of the load cell started recording data and displaying the real-time loading curves before the position control device drove the load cell in a 0.0005 inch/s (0.0127 mm/s) speed. The movements of the load cell were stopped at appropriate time judged from the loading curves. After that, both the axial loads and the lateral loads were withdrawn.

3. Compression Test Results

This section demonstrates the results of compression tests and discusses the influences of initial imperfections on the buckling load and path.

3.1 Buckling Path

The buckling paths of the cylinders are shown in Fig.9. Two tests for each shape of the cylinders are denoted in the same color.

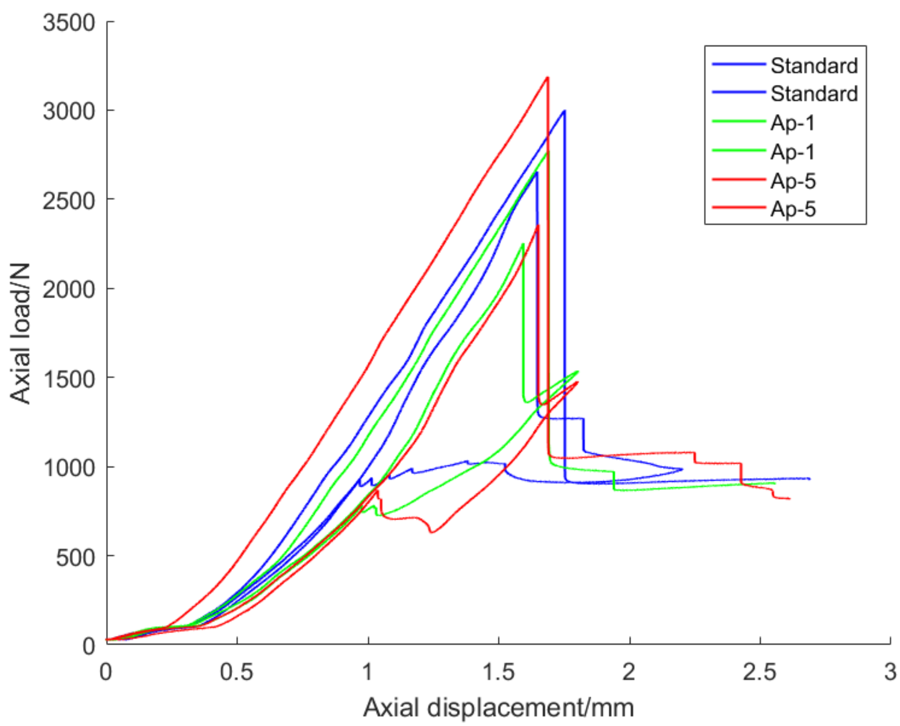

Figure 9: Buckling paths of cylinders in all tests

In the two tests for each shape, only one of them ran as a loading-unloading test. The positions of unloading were determined by the other only loading test. It can be seen that the drops of load exist in the post-buckling paths which means that the cylinders may switch into new mode shapes. So for the loading-unloading tests of Ap-1 and Ap-5, the unloading positions were set close to the buckling positions to keep each of them buckling in one mode shape. The beginning part of the buckling path has a different slope with the main linear part before the buckling for all cylinders because at the beginning part the end of shell and the end plate of testing machine might not respectively fit the V-shape groove and the top board perfectly enough.

It is clear that the repeatability of the compression tests is poor. Big discrepancies exist between different post-buckling paths and this is why the unloading position of the standard cylinder is set too far to limit the cylinder in one mode shape. The buckling loads are not identical either.

3.2 Buckling Load

The buckling loads of the cylinders are listed in Table.2 for a quantitative comparison. These loads are the peak loads before drops and captured directly from Fig.9.

The buckling loads in the loading-unloading tests are bigger than those in the loading tests in general. Inside each type of the test, the buckling load of Ap-1 is lower than that of the standard one at about 7% and 15% respectively, while the buckling load of Ap-5 can be either higher or lower than the standard one.

Table 2: Buckling loads of cylinders in all tests

	Buckling load in loading test (N)	Buckling load in loading-unloading test (N)
Standard	3001	2655
Ap-1	2774	2253
Ap-5	3188	2356

3.3 Role of Initial Imperfections

From the discussion above, it can be concluded that it is difficult to assess the influences of the designed initial imperfections on the buckling load and path due to the poor repeatability of the test results. The Ap-1 and Ap-5 imperfections are not the main effect in changing the buckling behavior and might be overridden by other unpredictable imperfections in the printing or testing process.

[5] shown that 3D printed cylindrical shells with buckling mode shapes imperfections, called SGI shells, were less sensitive to other imperfections and behaved more uniformly in compression tests. The buckling paths of SGI shells were clearly different from those of the standard shells. In the compression tests of this thesis, the buckling mode shapes was also observed and could be used to print new cylinders with buckling mode shapes imperfections. Compression tests on these cylinders may generate more meaningful results.

4. Poking Test Results

This section demonstrates the results of poking tests and discusses the influences of initial imperfections on the shape of the lateral force-displacement relationship.

Poking tests are more challenging than compression tests. Although they should be a non-destructive method as mentioned before, it was hard to control the displacement of the lateral poker in a range generating no damage to the cylinders at the first time of tests. Thus for some prescribed axial loads, only the results of one or two cylinder were obtained and more poking tests need to be done.

4.1 Lateral Path

The prescribed loads were chosen as 500 N, 900 N, 1500 N, 2000 N and 2500 N based on the buckling paths from the only loading compression tests. The lateral force-displacement relationships of cylinders under the 500 N prescribed load are shown in Fig.10. Two tests for each shape of the cylinders, with the difference of flipping the cylinders and poking at new positions, are denoted in the same color. The displacements are calculated based on the speed of the load cell and the time.

For the 500 N prescribed load, the results of all cylinders were obtained, though the two tests for each shape of the cylinders did not yield exactly same results. The lateral force increases slightly faster with the displacement before 1 mm as the amplitude of the imperfection increase. Same conclusion holds for 1 mm to 3 mm segment if the average of two results for each shape of cylinders are considered.

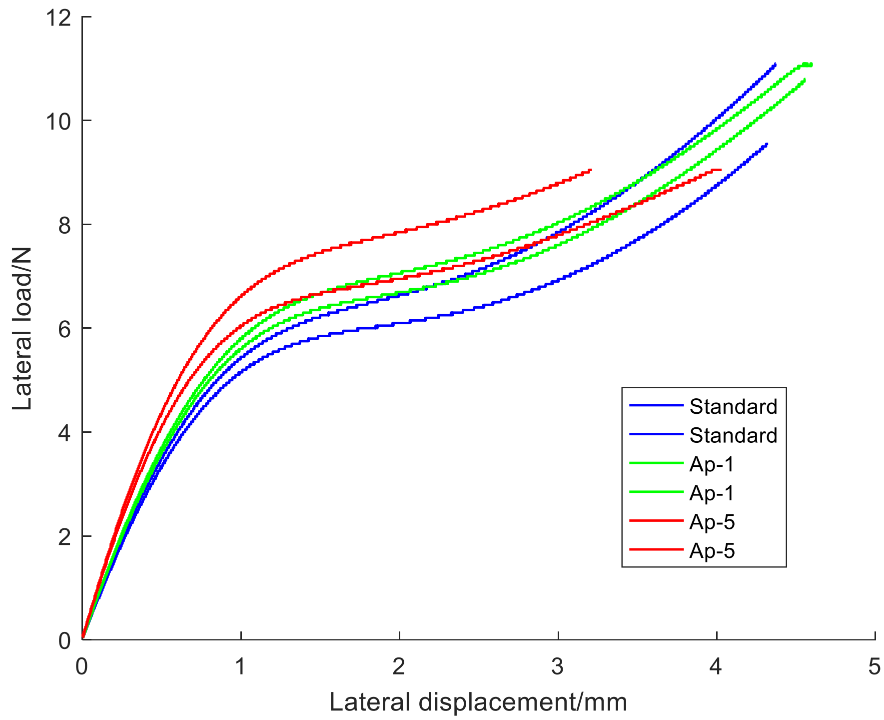

Figure 10: Lateral paths of cylinders under 500 N prescribed load

The lateral force-displacement relationships of cylinders under the 900 N and 1500 N prescribed load are shown in Fig.11. For these two loads, only the results of Ap-1 and Ap-5 were obtained since the standard cylinder was damaged during the poking process of the first test under 900 N. Color differentiates Ap-1 and Ap-5 and line type differentiates two prescribed loads.

For the 900 N and 1500 N prescribed load, the two tests on the same cylinder give same results at the beginning of the paths. According to [6] and [7], 900 N is closer to P_L of Ap-5 than that of Ap-1. Meanwhile 1500 N is closer to the buckling load of Ap-1 than that of Ap-5 if the average of two results for each shape are considered. This information will not be easily gained through compression tests and thus reveals the significance of poking tests in identifying the buckling behavior of cylinders and the influence of imperfections.

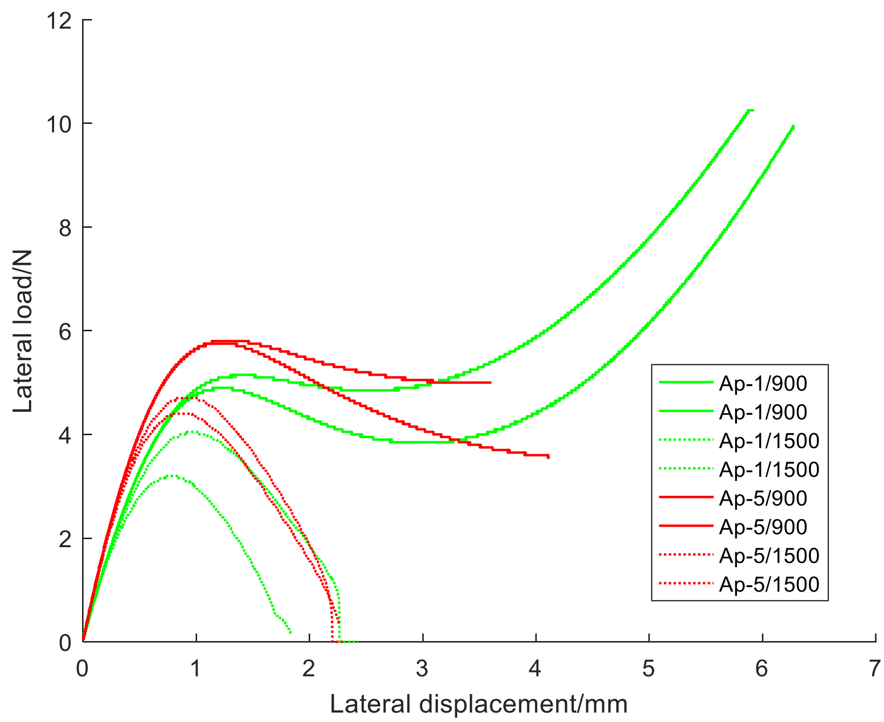

Figure 11: Lateral paths of cylinders under 900 N and 1500 N prescribed load

The lateral force-displacement relationships of cylinders under the 2000 N and 2500 N prescribed load are shown in Fig.12. For these two loads, only the results of Ap-5 were obtained since Ap-1 was damaged during the poking process of the first test under 2000 N. The two tests under 2000 N give almost same results. The small end displacement indicates that 2000 N and 2500 N are close to the buckling load of Ap-5.

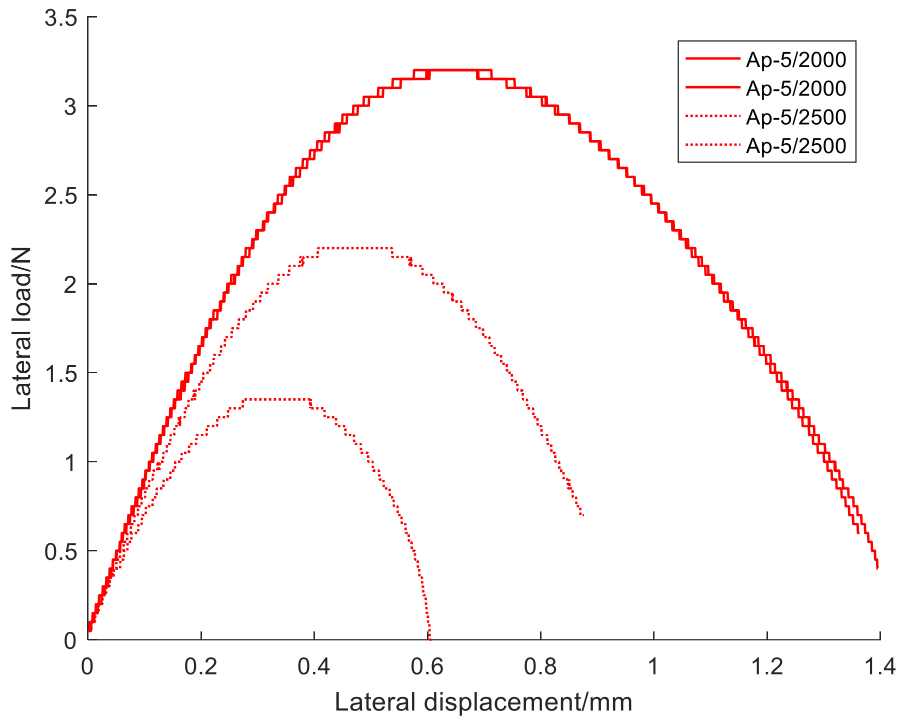

Figure 12: Lateral paths of cylinders under 2000 N and 2500 N prescribed load

4.2 Role of Initial Imperfections

Due to the lack of test results, the influences of the initial imperfections on the shape of the lateral force-displacement relationship are hard to fully determine, though the potential has been shown in the discussion on Fig.11. Yet as mentioned in 3.3, these influences are not necessarily generated by the designed imperfections. Cylinders with buckling mode shapes imperfections can be used for further study.

5. Conclusion

The poking test is a promising method to reveal the effect of imperfections on the buckling behavior of cylindrical shells. However, the role of designed initial imperfections, which are generated by half period sine-wave generatrixes with 1 mm and 5 mm amplitudes, are not clear because they might be overridden by other unpredictable imperfections. Only certain types of designed initial imperfections, such as buckling mode shapes imperfections may materially alter the buckling path and load.

References

[1] Chajes, Alexander. (1974). *Principles of Structural Stability Theory*. Prentice-Hall, Inc., Englewood Cliffs, New Jersey.

[2] Horak, Jiri., Lord, Gabriel J., & Peletie, Mark A. (2006). Cylinder Buckling: The Mountain Pass as an Organizing Center. *SIAM Journal of Applied Mathematics, 66*(5), 1793–1824.

[3] Hilburger, Mark W., Waters, W. Allen, Jr., & Haynie, Waddy T. (2015). Buckling Test Results from the 8-Foot-Diameter Orthogrid-Stiffened Cylinder Test Article TA01. https://ntrs.nasa.gov/search.jsp?R=20150017037

[4] Thompson, J. Michael T. (2015). Advances in Shell Buckling: Theory and Experiments. *International Journal of Bifurcation and Chaos, 25*(1), 1530001.

[5] Hu, Nan., & Burgueno, Rigoberto. (2015). Elastic Postbuckling Response of Axially-Loaded Cylindrical Shells with Seeded Geometric Imperfection Design. *Thin-Walled Structures*, 96, 256–268.

[6] Thompson, J. Michael T., Hutchinson, John W., & Sieber, Jan. (2017). Probing Shells Against Buckling: A Nondestructive Technique for Laboratory Testing. *International Journal of Bifurcation and Chaos*, *27*(14), 1730048.

[7] Virot, Emmanuel., Kreilos, Tobias., Schneider, Tobias M., & Rubinstein, Shmuel M. (2017). Stability Landscape of Shell Buckling. *Physical Review Letters,* 119, 224101.

[8] Karman, Theodore von., & Tsien, Hsue-Shen. (1941). The Buckling of Thin Cylindrical Shells under Axial Compression. *Journal of the Aeronautical Sciences, 8*(8), 303–312.

[9] Thurston, G. A., & Freelund, M. A. (1966). Buckling of Imperfect Cylinders under Axial Compression. https://ntrs.nasa.gov/search.jsp?R=19660022380